

MICROSTRUCTURE AND MECHANICAL PROPERTIES OF Al_2O_3 / A336 COMPOSITE BY LOW PRESSURE INFILTRATION

T. Harimoto¹, Y.B. Choi^{2*}, K. Matsugi² and G. Sasaki²

¹ Mechanical Science and Engineering, Graduate School of Engineering, Hiroshima University,
Higashi-Hiroshima, 739-8527, Japan

² Materials and Production Engineering, Faculty of Engineering, Hiroshima University,
Higashi-Hiroshima, 739-8527, Japan

(*Corresponding Author: ybchoi@hiroshima-u.ac.jp)

Keywords: *LPI(Low-pressure infiltration), Mechanical property, Alumina short-fiber*

1. Introduction

The ceramic fiber/whisker reinforced aluminum matrix composites have a considerable potential for providing light components exhibiting high specific strength with high specific stiffness excellent wear resistance, low thermal expansion and improved high temperature properties as compares with the conventional materials.

So they have many applications such as automotive parts, sports goods, robot parts, electrical parts and so on. However, it was considered difficult to use some of them in the civil industry because of the high cost of the reinforcement and processing [1] [2].

Alumina reinforced Al-alloy matrix composite that has well wear resistance and this composite can use the material of any parts to need high wear resistance such as cylinder bore, and optimum combination of pistons and piston ring [3].

The casting processes are recognized to be the most advantageous because of their high productivity and formability. High-pressure infiltration is one of the casting processes used for the fabrication of MMCs, but it has some disadvantages such as high cost arising from the preparation of preforms and large scale facilities for high pressure infiltration [4].

Low pressure infiltration process (LPI) has the advantage of being semi-automatic and thus reducing labor costs as well as obtaining a better casting quality and a higher yield. Cost of LPI is lower than that of squeeze casting and that the process provides a better quality than gravity casting [5].

In spite of its many advantages, LPI process has not yet been fully appreciated and as used as widely as it should [6].

Research of the microstructure around interface between reinforcement and matrix, and mechanical

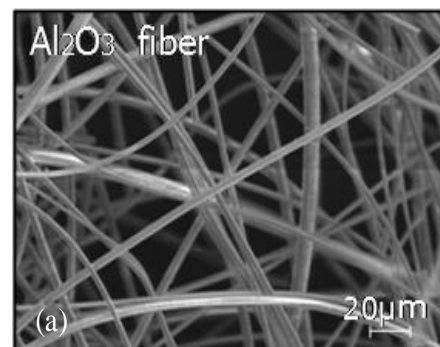
characteristic of alumina reinforced Al-alloy matrix composite that is fabricated by LPI process is not also fully.

This study clarifies the microstructure of interface between alumina fiber and the matrix, and their mechanical properties, including Young' modulus, indentation hardness and flexural strength were studied.

2 Experimental and procedure

Al_2O_3 short fiber (The Electro Chemical Industrial Ltd.) with diameter of $3.5\mu\text{m}$ and density of $3.55\text{Mg}/\text{m}^3$ was used for the reinforcement. Chemical composition of fiber is 97% Al_2O_3 and 3% SiO_2 .

Fig.1. shows the SEM images of Al_2O_3 fiber (a) and SiO_2 binder on the fiber surface of preform after sintering (b). SiO_2 binder adhered to the fiber surface by the thickness of $1\mu\text{m}$. In order to fabricate the preform, SiO_2 sol (snow-tech ZL, Nissan Chemical Industries, Ltd.) was used for binder and polyacrylamide (polystron705, Arakawa Chemical Industries, Ltd.) was used for coagulant. Volume fraction of preform is 10%. Matrix in this experiment was used A336 alloy, which composition is Al-12mass%Si-1mass%Ni-1mass%Cu-1mass%Mg.



| Report Documentation Page | | | | Form Approved OMB No. 0704-0188 | |
|--------------------------------------------------------------------------------------------------------------------------------------------------------------------------------------------------------------------------------------------------------------------------------------------------------------------------------------------------------------------------------------------------------------------------------------------------------------------------------------------------------------------------------------------------------------------------------------------------------------------------------------------------------------------------------------------------------------------------------------------------------------------------------------------------------------------------------------------------------|------------------------------------|-------------------------------------|------------------------------------------|------------------------------------------|---------------------------------|
| Public reporting burden for the collection of information is estimated to average 1 hour per response, including the time for reviewing instructions, searching existing data sources, gathering and maintaining the data needed, and completing and reviewing the collection of information. Send comments regarding this burden estimate or any other aspect of this collection of information, including suggestions for reducing this burden, to Washington Headquarters Services, Directorate for Information Operations and Reports, 1215 Jefferson Davis Highway, Suite 1204, Arlington VA 22202-4302. Respondents should be aware that notwithstanding any other provision of law, no person shall be subject to a penalty for failing to comply with a collection of information if it does not display a currently valid OMB control number. | | | | | |
| 1. REPORT DATE AUG 2011 | | 2. REPORT TYPE N/A | | 3. DATES COVERED - | |
| 4. TITLE AND SUBTITLE Microstructure And Mechanical Properties Of Al2o3 / A336 Compsite By Low Pressure Infiltratrion | | | | 5a. CONTRACT NUMBER | |
| | | | | 5b. GRANT NUMBER | |
| | | | | 5c. PROGRAM ELEMENT NUMBER | |
| 6. AUTHOR(S) | | | | 5d. PROJECT NUMBER | |
| | | | | 5e. TASK NUMBER | |
| | | | | 5f. WORK UNIT NUMBER | |
| 7. PERFORMING ORGANIZATION NAME(S) AND ADDRESS(ES) Mechanical Science and Engineering, Graduate School of Engineering, Hiroshima University, Higashi-Hiroshima, 739-8527, Japan | | | | 8. PERFORMING ORGANIZATION REPORT NUMBER | |
| 9. SPONSORING/MONITORING AGENCY NAME(S) AND ADDRESS(ES) | | | | 10. SPONSOR/MONITOR'S ACRONYM(S) | |
| | | | | 11. SPONSOR/MONITOR'S REPORT NUMBER(S) | |
| 12. DISTRIBUTION/AVAILABILITY STATEMENT Approved for public release, distribution unlimited | | | | | |
| 13. SUPPLEMENTARY NOTES See also ADA555447. International Conference on Composite Materials (18th) (ICCM-18) Held in Seoul, Korea on August 22-26, 2011. U.S. Government or Federal Purpose Rights License | | | | | |
| 14. ABSTRACT | | | | | |
| 15. SUBJECT TERMS | | | | | |
| 16. SECURITY CLASSIFICATION OF: | | | 17. LIMITATION OF ABSTRACT SAR | 18. NUMBER OF PAGES 4 | 19a. NAME OF RESPONSIBLE PERSON |
| a. REPORT unclassified | b. ABSTRACT unclassified | c. THIS PAGE unclassified | | | |

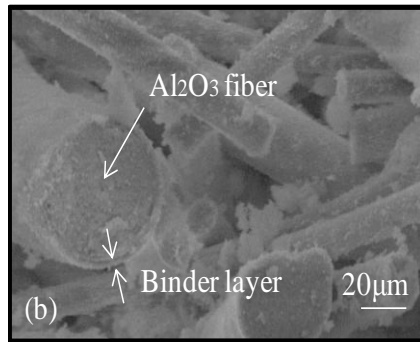


Fig.1. SEM images of Al₂O₃ fiber (a), fiber and SiO₂ binder inside preform (b)

Fig. 2 shows a schematic of the low-pressure infiltration experimental apparatus. The preform was fixed at the bottom. Molten alloy was infiltrated to the upper part of the preform. The pressure of 0.4MPa and 0.7MPa was applied to the molten alloy. The environment controls the vacuum and the atmosphere respectively, and the temperature of molten alloy is 1173K.

Microstructure of interface between alumina fiber and the matrix was observed by FE-SEM (HITACHI S-5200) and SEM (HITACHI S-5000). Map analysis and point analysis of interface between fiber and matrix carried out by EDS (EDAX JAPAN Genesis XM2) and XRD (Mac Science M03XHF22).

In additions, indentation hardness and Young's modulus of interface between fiber and matrix carried out by nano indentation test (ELIONIX ENT-1100a). Depth sensing indentation tests carried out using a diamond Berkovich indenter. Load was performed the constant of 30mN. Finally, flexural test carried out to observe an interfacial fracture behavior. The flexural property was evaluated by three point test method (ASTM C-1341).

3 Results and discussion

3.1 Microstructural analysis

Fig.3 shows the SEM images and EDS analysis of Al₂O₃ fiber and SiO₂ binder, Fig.4 shows the XRD results of Al₂O₃/A366 composite and matrix.

As seen Fig.3.(A), Al₂O₃ fiber was random distribution in matrix and interfacial layer (SiO₂ binder) between reinforcement and matrix was observed at from Fig.4. (B). Interfacial layer is very clear and bonds directly with matrix and fiber. It is confirmed by the presence of the γ -Al₂O₃, MgO from diffraction peaks in the XRD pattern (Fig 4) and EDS (Fig. 3(b),(c)). It suggests that γ -Al₂O₃, MgO can be produced as results of the interfacial reaction between the Al liquid and the SiO₂ binder, i.e. $4Al + 3SiO_2 \rightarrow \gamma-Al_2O_3 + 3Si$, $2Mg + SiO_2 \rightarrow 2MgO + Si$, which results in improved interfacial wettability [7]

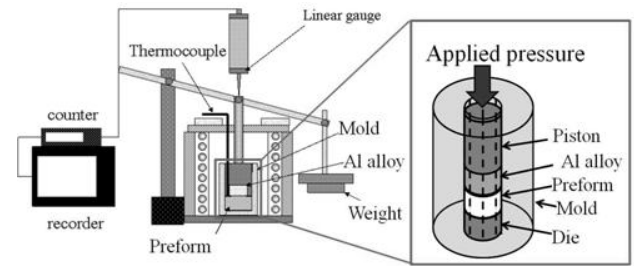


Fig. 2. Apparatus for LPI experiments

and leads to an improvement in the bonding strength of the interface and the mechanical properties of composites.

Al₂O₃ fiber is also confirmed by the presence of the MgAl₂O₄ from diffraction peaks in the XRD pattern (Fig 4) and EDS (Fig. 3(a)). It suggests that MgAl₂O₄ can be produced as results of the reaction between the α -Al₂O₃ and the MgO, i.e. $\alpha-Al_2O_3 + MgO \rightarrow MgAl_2O_4$. It was noticed that MgAl₂O₄ improve wettability, but decrease mechanical properties by age hardening [8]

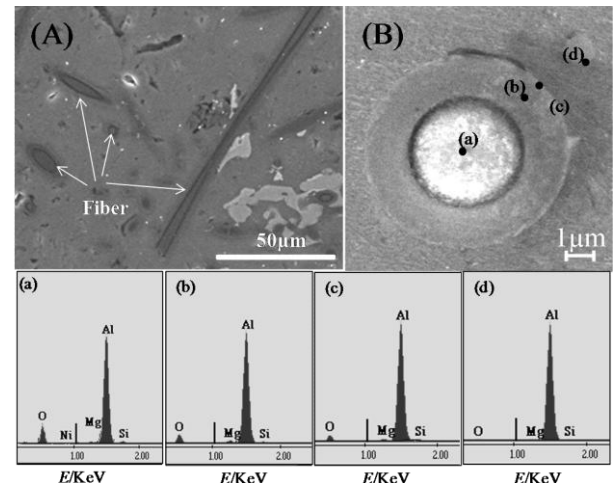


Fig. 3. SEM images of cross section(A), interfacial layer between fiber and matrix(B) and EDS results of each position.

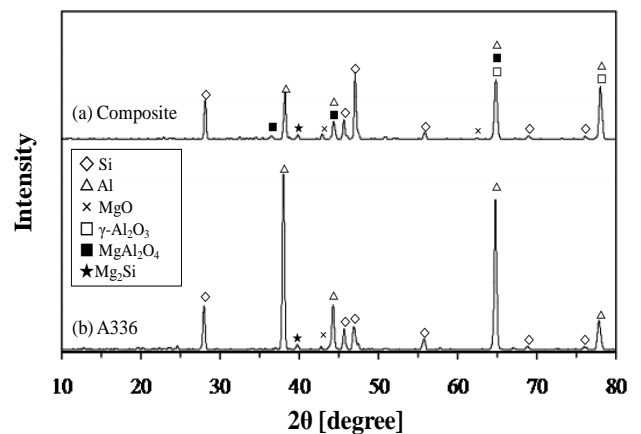


Fig. 4. Result of XRD (a) Al₂O₃/A366 composite and (b) matrix.

3.2 Indentation hardness

Fig.5. shows the result of load - displacement curves of each position in the composites. The load-displacement curves are related to the elastic modulus and hardness of work materials.

Load-displacement curves the fiber (a), interface between fiber and the interfacial layer (b), interface between fiber and the interfacial layer (d) shows a higher gradient compared with interfacial layer (c) and matrix (e). It seems that the fiber (a), interface between fiber and the interfacial layer (b), interface between fiber and the interfacial layer (d) increase the Young's modulus and decrease plasticity compared with interfacial layer (c), matrix (e).

Fig.6. shows the Young's modulus and indentation hardness of each position of composite.

Young's modulus of the matrix shows the same result as the reference value [9]. However, Young's modulus of Al_2O_3 fiber was considerably low comparison with Young's modulus of Al_2O_3 which has 300GPa [10]. That is the same value with $MgAl_2O_4$ have 182GPa [11]. Therefore, Al_2O_3 short fiber changed to $MgAl_2O_4$ that produced from chemical reaction ($\alpha-Al_2O_3 + MgO \rightarrow MgAl_2O_4$).

Indentation hardness is the same tendency as Young's modulus.

3.3 Flexural strength

Specimen of $3W \times 1T \times 26L$ mm with support span of 16mm was applied to the 3 point bending test. 3 point bending test carried out the cross head speed of 0.5mm/min. Composite was fabricated by applied pressure from 0.4MPa to 0.7MPa. Temperature of molten alloy is 1173K. The environment controls the vacuum and the atmosphere respectively.

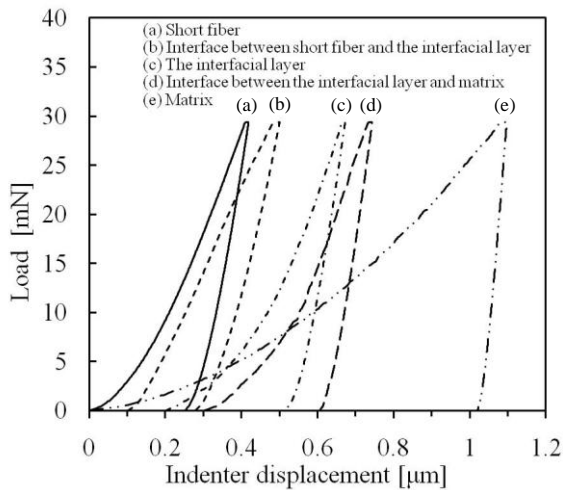


Fig.5. Indentation load versus displacement of (a) fiber (b) interface between fiber and the interfacial layer (c) the interfacial layer (d) interface between fiber and the interfacial layer (e) matrix.

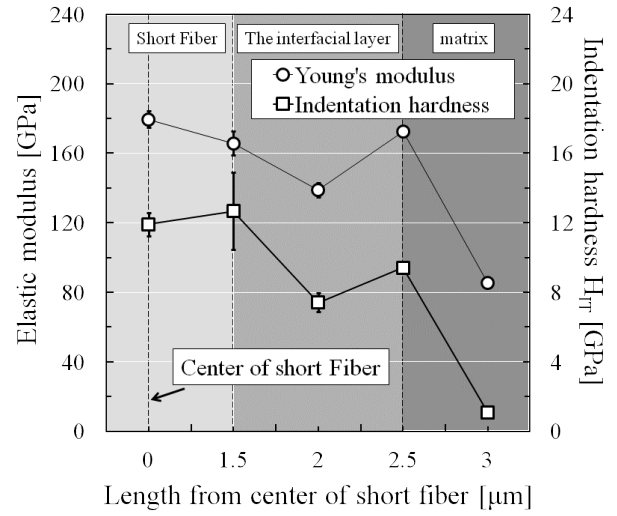


Fig.6. Young' modulus and indentation hardness from each position.

Fig.7. shows the result of relationship flexural strength and relative density for each condition. The relative density increases when applied pressure increases. The Al_2O_3 reinforced A366 composite of the relative density 99% was fabricated under applied pressure of 0.7MPa and in the vacuum.

Flexural strength of the composite that the fabrication condition was made by applied pressure of 0.4MPa and in air is 226.21 ± 12.36 MPa. Flexural strength of the composite that the fabrication condition was made by applied pressure of 0.7MPa and in air is 246.34 ± 1.89 MPa. Flexural strength of the composite that the fabrication condition was made by applied pressure of 0.7MPa and in vacuum is 276.85 ± 12.41 MP. Flexural strength of the composite fabricates by applied pressure, 0.7MPa and vacuum was the highest compared to other composites.

Fig. 8 shows the dependency of flexural strength for relative density. However, when the relative density

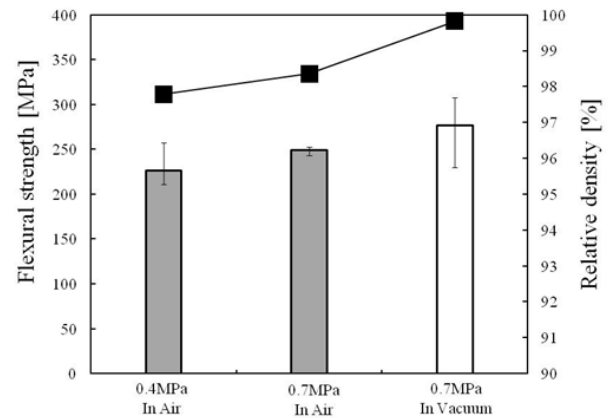


Fig.7. Result of relationship flexural strength and relative density.

was 99%, flexural strength has increased by 35% or more compared with the matrix (192MPa [12]).

Fig.9. shows SEM image of fracture surface of 3 point bending test specimen. The crack propagation around fiber was observed from the fracture surface. Almost crack was propagated to the interface between fiber and the interfacial layer, between interfacial layer and the matrix. The crack was observed to propagate in the interface with low hardness and low Young's modulus.

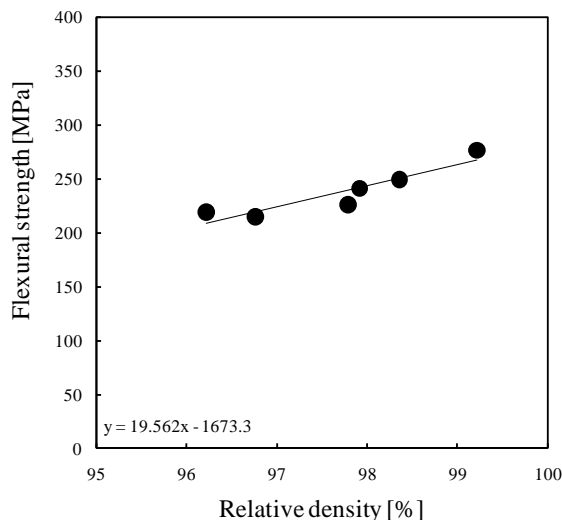


Fig.8. Relationship of flexural strength and relative density of $\text{Al}_2\text{O}_3/\text{A366}$ composite.

4. Conclusions

This paper clarifies the microstructure and mechanical properties of interface between alumina fiber and the matrix. The important results are listed below.

1) SiO_2 binder is very clear and bonds directly with matrix and fiber. SiO_2 binder layer was changed to the $\gamma\text{-Al}_2\text{O}_3$, MgO by the reaction between the Al liquid and the SiO_2 binder. MgAl_2O_4 was also confirmed in the Al_2O_3 fiber. Fiber was changed to the MgAl_2O_4 by reaction between the $\alpha\text{-Al}_2\text{O}_3$ and the MgO .

2) Young's modulus and indentation hardness of each position has the same value of MgAl_2O_4 , $\gamma\text{-Al}_2\text{O}_3$, MgO . Almost crack was propagated to the interface between fiber and the interfacial layer, between interfacial layer and the matrix. The crack was observed to propagate in the interface with low hardness and low Young's modulus.

Reference

- [1] L. Yao, G. Sasaki and H. Fukunaga "Reactivity of aluminum borate whisker reinforced aluminum alloys". *Materials Science and Engineering A*, Vol. 225, pp 59-68, 1997.
- [2] T. Yamanaka, Y.B. Choi, O. Yanagisawa and G. Sasaki "Influence of preform preparation condition on infiltration of molten aluminum". *Jour. of Mater. Pro. Tech.*, vol. 187-188, pp 530-532, 2007.
- [3] K. Shibata and H. Ushio "Tribological application of MMC for reducing engine weight". *Tribology Inter.*, Volume 27, Issue 1, February, pp 39-44, 1994.
- [4] M. Mizumoto, T. Ohgai and A. Kagawa "Characterization of fiber-reinforced metal matrix composites fabricated by low-pressure infiltration process". *Materials Science and Engineering A*, Vol. 413-414, pp 521-526, 2005.
- [5] R. Ashiri, B. Niroumand, F. Karimzadeh, M. Hamani and M. Pouranvari "Effect of casting process on microstructure and tribological behavior of LM13 alloy". *Journal of Alloys and Compounds*. Vol.475, pp 321-327, 2009.
- [6] Y.B. Choi, G. Sasaki, K. Matsugi, N. Sorida, S. Kondoh, T. Fujii and O. Yanagisawa "Simulation of infiltration of Molten Alloy to Porous Preform Using Low Pressure". *JSME International Journal A*, Vol. 49, No.1, pp20-24, 2006.
- [7] Z.Q. Yu, G.H. Wu, D.L. Sun and L.T. Jiang "Coating of Y_2O_3 additive on Al_2O_3 powder and its effect on the wetting behavior in the system $\text{Al}_2\text{O}_3/\text{Al}$ ". *Materials Letter*, Vol.57, pp 3111-3116, 2003.
- [8] Y. Tomota, T. Ohnuki, M. Huang, Y. Ichinose, H. Ohta and Y. Takeuchi "Application of powder liquid forging technique to fabrication of Al_2O_3 or SiC particle / 6061 Aluminum alloy metal matrix composites and their mechanical properties". *Journal of Japan institute of light metals*. Vol.43, No.4, pp 213-218, 1993.
- [9] T. Sato "Metallographic and Characteristic of Aluminum". 1st edition, The Japan Institute of Light Material, 1991.
- [10] A.R. Bunsell "Oxide fibers for high-temperature reinforcement and insulation". *Metals and Materials Society*, Vol.57, No.2, pp 48-51, 2005.
- [11] A.K. Kushwaha "Vibrational and elastic properties of aluminate spinel MgAl_2O_4 ". *Physica B*. Vol. 405, pp 2795-2798, 2010.
- [12] K. Usuda "Ceramics fiber to which diameter under $30\mu\text{m}$ used for FRM and which removed carbon element of textile surface". P2000-404638, 10, 07, 2002.

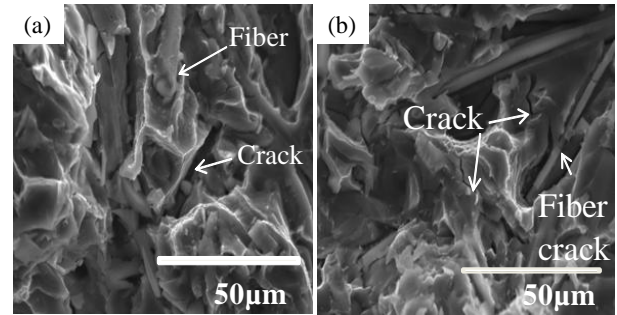


Fig.9. SEM images of fracture surface of $\text{Al}_2\text{O}_3/\text{A336}$ composite.